Comparison of intravenous coronary angiography using synchrotron radiation with selective coronary angiography

W.-R. Dix,[a]* W. Kupper,[b] T. Dill,[c] C. W. Hamm,[c] H. Job,[d] M. Lohmann,[a] B. Reime[a] and R. Ventura[d]

[a]Hamburger Synchrotronstrahlungslabor HASYLAB at DESY, Notkestrasse 85, D-22607 Hamburg, Germany, [b]Herz-Kreislauf-Klinik Bevensen, Department of Cardiology II, Römstedter Strasse 25, D-29549 Bad Bevensen, Germany, [c]Kerckhoff-Klinik, Department of Cardiology, Benekestrasse 2-8, D-61231 Bad Nauheim, Germany, and [d]Universitäts-Krankenhaus Hamburg-Eppendorf, Department of Cardiology, Martinistrasse 52, D-20251 Hamburg, Germany.
E-mail: wolf-rainer.dix@desy.de

Intravenous coronary angiography with synchrotron radiation is a novel and minimally invasive technique for coronary imaging. At the Hamburger Synchrotronstrahlungslabor HASYLAB at DESY, a dedicated angiography system has been developed, which has been shown to provide detailed images of coronary artery segments. For each scan, two monochromatic X-ray images below and above the *K*-edge of iodine were recorded simultaneously. The two images were subtracted logarithmically to produce a maximal contrast enhancement of the iodine. To date, the procedure has been carried out on 379 outpatients. No complications occurred during or after the angiographic procedure, and hospitalization was not required in any subject. The acceptance by patient is extremely high. Five outside reviewers, blinded as to the clinical data or prior angiographic interpretation, reviewed the images for the presence or absence of 70% or more occlusion of a vessel. They reached a sensitivity of 79% and a specificity of 99%. The study has demonstrated that the synchrotron method has satisfactory sensitivity and very high specificity for severe stenoses. The new method has several advantages over magnetic resonance imaging (MRI), electron beam computed tomography (EBCT), and multi-slice computed tomography (MSCT). Neither vascular calcification (CT) nor the presence of metal stents (MRI) impairs the evaluation of perfusion of segments of the coronary arteries. Furthermore, the spatial resolution is three or four times higher using synchrotron angiography, and problems due to respiratory motion are eliminated.

Keywords: coronary artery disease; intravenous coronary angiography; minimally invasive technique; dichromography; human studies.

1. Introduction

Selective coronary arteriography is the standard of reference for the imaging of coronary anatomy and for establishing the presence, site and severity of coronary artery stenoses (narrowings; for explanations of medical terms see Appendix *A*). The technique is widely available and, for example, in 1999 in Germany, 561 623 procedures were performed (Mannebach *et al.*, 2000). However, the procedure is invasive (involving the insertion of a catheter into an artery) and expensive, causes inconvenience to the patients, and carries a small risk because of the associated complications.

Therefore, efforts have been made to image coronary arteries, coronary stents and bypass grafts without risk and in an ambulatory way by non-invasive or minimally invasive methods (*i.e.* methods that do not involve inserting a catheter into the arteries). One such method is dichromography after the intravenous injection of a contrast agent. Dichromography is not a slice technique, unlike competing methods, such as magnetic resonance imaging (MRI), electron beam computed tomography (EBCT) or multi-slice computed tomography (MSCT).

The first studies of intravenous synchrotron-radiation iodine-dichromographic coronary angiography were performed on human subjects at the Stanford Synchrotron Radiation Laboratory (SSRL) in 1986 (Rubenstein *et al.*, 1986). At the same time, at the Hamburger Synchrotronstrahlungslabor HASYLAB, the NIKOS system was developed for this intravenous technique. The development of this system was successfully completed in 2000. In the same year, similar studies commenced at the European Synchrotron Radiation Facility (ESRF) in Grenoble, France (Elleaume *et al.*, 2000). Another synchrotron-radiation system, which differs considerably from the others, is in operation at the Photon Factory, KEK, in Tsukuba, Japan (Ohtsuka *et al.*, 1999), and a further system is planned for implementation in Shanghai, China (Shanghai National Synchrotron Radiation Center, 1999).

To date, 379 outpatients have been investigated with the NIKOS system. Although this number includes several studies with changing protocols and systems, all of these patients got a final diagnosis. The latest and largest study, with a fixed protocol and an unchanged system (version IV), involved 230 patients and is described in this paper. The method was compared with selective coronary angiography to assess the diagnostic accuracy of the new intravenous method, with the conventional selective coronary angiography method taken as the reference standard.

2. Methods

2.1. Dichromography

Dichromography is a special form of digital subtraction angiography that greatly enhances signals of low contrast (Dix, 1995; Jacobson, 1953). The digital subtraction is based on the logarithmic subtraction of two images recorded at different energies (Fig. 1), using the discontinuity at the absorption *K*-edge of the iodine-containing contrast agent at 33.17 keV (E_K). The two images are obtained simultaneously with monochromatic X-rays just below (E_1 = mask) and above (E_2 = image) the *K*-edge. For an energy separation of ≤ 300 eV and a bandwidth of the monochromatic X-ray beams of ≤ 250 eV, the change in the mass absorption coefficient for iodine between E_1 and E_2 is about 10000 times higher than the change for soft tissue. Therefore, the contrast enhancement due to the subtraction allows the visualization in coronary arteries of 1 mm diameter of a very low contrast of iodine, down to a mass density of 1 mg cm^{-2}. This corresponds to a dilution of the contrast agent by a factor of 40. Because, in the dichromography method, the two images are taken simultaneously, it is possible to freeze the motion of fast-moving small structures, such as the coronary arteries after peripheral intravenous injection, without the introduction of a catheter.

2.2. NIKOS system

The method requires monochromatic X-ray beams of between 2×10^{11} and 15×10^{11} photons s^{-1} mm^{-2}, the exact number depending on the protocol of the investigation. Currently such an intensity is available only at synchrotron-radiation sources. Therefore, the NIKOS system was installed at the storage ring DORIS at DESY in Hamburg, Germany.

The development of the NIKOS system was a continuous process. Version IV of the system was installed at the end of 1996. The NIKOS(IV) system is more advanced than those at NSLS (USA), ESRF (France) or KEK (Japan) because its detector has an extreme high dynamic range of 300000:1 at a very low equivalent photon noise of 7.6 photons, a high detective quantum efficiency of 85% and no bad channels. Furthermore, the optics of the system allow a scanning time of 250 ms and, therefore, ECG-triggered imaging.

The NIKOS system was designed as a line-scan system to reduce background scattering in images and to optimally match the conditions of a beamline at a storage ring. It is described in detail elsewhere (Dill *et al.*, 1998). The principal components of the system are as follows (Fig. 2):

(i) A monochromator (Illing *et al.*, 1995), which comprises two bent Si(111) crystals in a Laue geometry and which filters the two monochromatic beams, each 13 cm wide and 0.5 mm high. The monochromated beams cross at the position of the patient's heart.

(ii) A safety system equipped with three independent ultra-fast shutters, which close in less than 10 ms in response to any event that might increase the dose to the patient or the physician.

(iii) A hydraulic scanning device that drives the patient's chair up and down. It is ECG-triggered, and the chair is positioned so that the monochromatic beams are available over a vertical distance of 20 cm. The patient's chair seat rotates through $\pm 180^\circ$ around the vertical axis [left anterior oblique (LAO) and right anterior oblique (RAO) projections] and $\pm 20^\circ$ around the horizontal axis [caudiocranal (CC) projection].

(iv) A detector, which is a very fast low-noise two-line ionization chamber (Lohmann *et al.*, 1998; Lohmann, Besch *et al.*, 2003) that simultaneously records the two monochromated beams. The dynamic range of the complete detector system (300000:1) can be adjusted in four levels to suit the absorption of the patient. Each line has 336 pixels with 0.4 mm pitch and is recorded within 0.8 ms. These parameters allow the completion of an image scan of 320 lines within 250 ms. This scan allows the identification of low-contrast iodinated structures, of size 1 mm, in front of large iodinated structures such as the aorta, the left ventricle, lung tissue and bones.

(v) The software program, which provides a diagnosis a few minutes after the procedure (Jung *et al.*, 1999).

Measurements of ionization chambers inside the safety system are used to predict the dose to the patient, and the physician must approve the dose before the imaging procedure commences. The dose is also measured with thermoluminescence dosimeters (TLD) on the patient's chest. Although the skin-entry dose rate is as high as 64 Sv s^{-1}, the measured maximal skin-entry dose to the patient for the complete study is 220 mSv and in most cases does not exceed 110 mSv. This compares favorably with the mean skin-entry dose of 410 mSv for conventional selective coronary angiography. Following international rules it was calculated that for the NIKOS system the maximal effective dose for a complete study is 2.2 mSv for males and 4.4 mSv for females (ICRP, 1990).

2.3. Patients

The fixed-protocol study described here involved 230 patients. The goal of the study was to determine the sensitivity, specificity and predictive values of intravenous synchrotron-radiation coronary angiography compared with selective coronary angiography (Dill *et al.*, 2000). The study protocol was approved by the ethics committee of the Hamburg Medical Board, and to enter the study the patients were required to give written informed consent. Patients who were not thought to be able to sit in an upright position for at least 15 minutes and those with unstable angina pectoris (heart pain) were excluded from the study. All patients had anti-anginal and low-dose aspirin medication (medication against chest pain).

The sex distribution was 88% male and 12% female. Ages ranged from 36 to 81 years [mean = 61 ± 9 years], weights from 50 to 120 kg [mean = 81 ± 12 kg] and bodymass index (weight × height^{-2}) from 18.8 to 36.2 kg m^{-2} [mean = 26.5 ± 3.2 kg m^{-2}]. Because the absorption length of 33 keV photons in soft tissue is only 2.1 cm, and the skin-entry dose was fixed, the image quality varied with the size of the thorax. Nevertheless patients with a large thorax size were not excluded. The range in thorax diameters was 15–32 cm [mean = 23 ± 4 cm] in the sagittal axis, 28–53 cm [mean = 43 ± 4 cm] in the frontal axis and 82–126 cm [mean = 104 ± 8 cm] in circumference.

All patients were investigated as outpatients (ambulant). All but four had known coronary artery disease, with recurring symptoms. Eighty of the 230 patients (35%) had single-vessel disease (disease in one coronary artery), 56 (24%) had two-vessel disease and 90 (39%) had three-vessel disease. Ninety-two of the 230 patients (40%) had previous myocardial infarction, and 53 patients (23%) had undergone

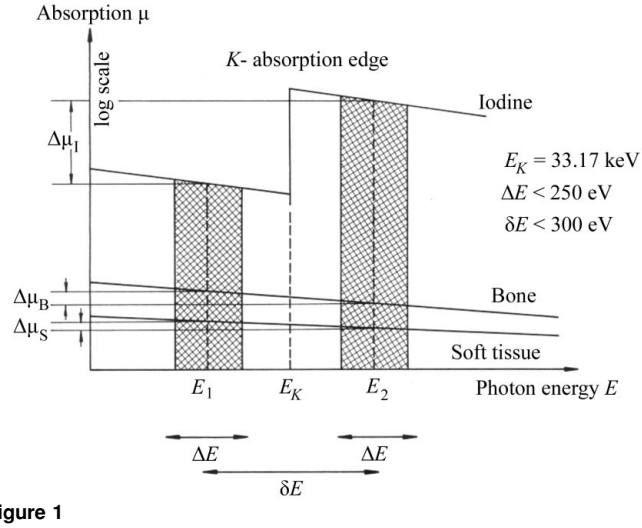

Figure 1
The difference in absorption at the *K*-edge of iodine is used to enhance the contrast of iodine by logarithmic subtraction. E_K is the energy at the *K*-edge (33.17 keV), E_1 is the energy of the monochromatic X-ray beam below the *K*-edge, E_2 is the energy above the *K*-edge, ΔE is the bandwidth of the two monochromatic beams, δE is the energy separation of the two monochromatic beams, $\Delta\mu_I$ is the difference of the absorption coefficient of iodine for X-rays above and below the *K*-edge, $\Delta\mu_B$ is the difference of the absorption coefficient of bone, and $\Delta\mu_S$ is the difference of the absorption coefficient of soft tissue.

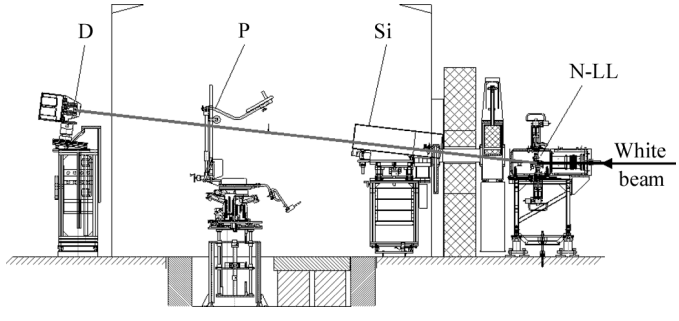

Figure 2
A schematic view of the NIKOS IV system. N-LL is the monochromator, Si the safety system, P the scanning device and D the detector.

bypass surgery [bypass grafts such as an aorto coronar vein bypass (ACVB) and/or an aorto coronar bypass with the internal mammary artery (IMA-ACB)]. One hundred and sixty-five (72%) were post intervention [percutaneous transluminal coronary angioplasty (PTCA; widening with the help of a balloon) or rotational atherectomy (high-speed rotating catheter)], and 118 (72% of those with interventions) had one to four stents (tubes of mashed metal). One patient was post coronary angiography without intervention, and seven patients had not undergone prior coronary angiography or intervention but were investigated because they refused selective coronary angiography. In five patients, intravenous infusion was technically impossible.

There were 609 target vessels examined in the 225 patients: 218 left anterior descending coronary arteries (LAD; 35% of the target vessels) including side branches, 150 right coronary arteries (RCA; 25%), 133 circumflex coronary arteries (Cfx; 22%) and 108 ACVB/IMA-ACBs (18%).

2.4. Image acquisition

In most cases two almost perpendicular projection angles were selected for each patient, which resulted in 450 injections of contrast agent in this study.

Under fluoroscopic control, 6F or 7F introducer sheaths (plastic cannula) were placed in the brachial vein (vein in the arm). In 40 injections (9%), a 4F, 6F or 7F pigtail catheter was advanced into the superior vena cava (central vein) to avoid excessive dilution of the contrast agent. These catheters were used in patients with an ejection fraction of $\leq 30\%$ (output of left ventricle) or a transit time of ≥ 20 s (time between injection and arrival). These catheters were also used, in 27 patients, for the second injection, if the first injection resulted in poor image quality because of a large bodymass index or a low flow from the peripheral to the central veins.

The patient was placed on the scan seat in an upright position, with raised arms to eliminate overlap problems, and was aligned to the X-ray beam with the aid of a light frame. The image session was performed in three steps:

(i) The individual transit time was determined as follows: 5 ml of indocyanine green (green organic fluid) were injected as an intravenous bolus *via* the introducer sheath. A sensor at the patient's scaphoid fossa of the external ear and a densitometer for visible light were used to determine the time between the injection of the dye and its arrival in the ear. The time at a quarter of the rise of the measured bolus in the ear corresponded experimentally to the transit time of the maximum of the contrast bolus to the coronary arteries. The transit times ranged from 5.5 to 24.8 s (mean = 14.7 $\pm$ 2.9 s).

(ii) To verify that the region of interest was included in the image and to confirm the measured transit time, a scout image was taken. The skin-entry dose to the patient was reduced to 10 mSv by the use of lucite absorbers, and only 5 ml of contrast agent were injected. In very rare cases a second scout image must be taken after the vertical and/or horizontal adjustment of the patient's seat.

(iii) After an interval of at least 5 min to allow the washout of the contrast agent and the adjustment of the patients's position, the diagnostic procedure was run using two to four scans; in most cases three scan images were recorded. The NIKOS system was adjusted to permit a total skin-entry dose of 100 mSv, irrespective of the number of scans and the patient size. For brachial vein injection, 30–40 ml (in most cases 30 ml) of contrast agent with 370 mg ml^{-1} of iodine were injected at a rate of 15 ml s^{-1} with a clinical injection pump. For superior vena cava injections, the same volume of 400 mg ml^{-1} contrast agent was injected at a rate of 15–20 ml s^{-1} (in most cases 18 ml s^{-1}). The scanning device operated at a speed of 50 cm s^{-1} and took one scan image on each scan, whether the device was running up or down. Therefore, the time interval between the scans is about 2 s and the patient's period of breath holding did not exceed 8 s. The procedure was initiated by ECG triggering, and the fast shutters in the safety system were opened only as long as the field of interest moved through the monochromatic X-ray beams. The scans were taken in endsystolic phase (center of the image 225 ms after the *R*-wave; time interval 100–350 ms after the *R*-wave) to avoid superpostion on large iodinated structures such as the left chambers. One scan was completed in 250 ms, but because the delay within the two simultaneously recorded images from line to line is only 0.8 ms there were no motion artefacts. The dimensions of the scan images were 13.4 cm $\times$ 12.8 cm, with a pixel size of 0.4 mm $\times$ 0.4 mm. The spatial resolution was 11 line pairs per centimeter. The subtraction images were available to the physician 10 s after the procedure was completed. The complete set of filtered images was available after 3–5 min (Jung *et al.*, 1999).

Because even a small iodine background can degrade the image quality, the second run, with two to four scans taken at a different projection angle, is recorded after an interval of at least 30 min. During this 'down time', an imaging procedure can commence with another patient. Ordinarily, the final diagnosis after two investigation runs at different projection angles is completed within 10 min. Therefore, a complete examination of a patient lasts about 1 h.

The optimal projection angles for the target vessels differ slightly for intravenous *versus* intra-arterial selective coronary angiography. For the RCA, a LAO 30–45° projection is optimal, where the angle depends on the location of the diaphragms, with a slight craniocaudal angulation of 10°. The LAD was best imaged in the RAO 30–45° projection, again with a slight craniocaudal angulation of 5–10°. Segments of the Cfx or their marginal branches and the left main were overlapped by the left atrium, left ventricle or aorta in the LAO 60° and RAO 30–45° projections. The optimal angles for ACVBs are the same as those for the native arteries, and for an IMA-ACB the RAO 30° projection is preferred.

2.5. Image evaluation

During the final diagnostic evaluation, the physician analyzes the images interactively at a workstation (Alphastation 400 4/233). For each scan of the two infusion procedures, a complete set of images is prepared by the computer program. This set contains the two images at energies below and above the *K*-edge, a subtraction image, an iodine image, and unsharp-masking images of the subtraction and iodine images (Jung *et al.*, 1999).

The energy images are calculated from the stored raw data after correction for irregularities of the scanning device, intensity fluctuations of the monochromatic X-ray beams, and fixed-pattern noise and dark current of the detector system. The total noise from the system, from the electronics and from the image-acquisition procedure should not exceed 0.3%, thus ensuring a signal-to-noise ratio of ≥ 7 for a coronary artery whose diameter is 1 mm.

A simple pixel-by-pixel logarithmic subtraction of the energy images results in the subtraction image.

The iodine images are also calculated from the energy images. In this calculation, as in the dual-energy method, two images at different energies allow the separation of two elements with different atomic number, *Z*. In our case iodine and 'tissue' are separated, where 'tissue' includes water and bone. The calculation requires an iteration process for suppressing the beam-hardening effects from 99 keV photons. The monochromatic 33 keV X-ray beams contain 0.6% of

these higher harmonics. The iodine images provide quantitative values for the measured mass density of the iodine, which is important for quantitative coronary angiography.

To markedly improve the visualization of small structures, such as the coronary arteries, the images are filtered *via* the unsharp masking technique (Zeman, 1991). The original image (subtraction or iodine) is filtered with a median filter, in most cases with a filter radius of 15 pixels. The resulting median image is subtracted from the original image. For orientation purposes, the unsharp masking image can be mixed interactively with the original image in any optimal relation. These unsharp masking images improve the visualization of the ostium (entrance) of the RCA, the left main, if superposed by the aorta, and the Cfx in the segments that are superposed by the left ventricle.

The clinician can work on this presented image set, for example, with different gray-level adjustment methods, histogram equalization, and special software tools for stent presentation, for artefact processing or to follow the temporal course of the opacification of the vasculature. The two investigation runs can also be used to view the region of interest from two projection angles. This kind of image evaluation requires that the clinician be experienced in the interpretation of intravenous coronary angiograms, which is different from the interpretation of selective intracoronary angiograms.

After completion of the study, the images and data for all 225 patients were analyzed for possible improvements in the method.

Sixty of the 225 patients had intravenous coronary angiography as well as selective coronary angiography within eight weeks. The images of these patients were used for an intra-individual comparison of the methods and thus an assessment of the intravenous technique.

The intravenous angiograms of these 60 patients were presented to five cardiologists who were blinded as to the findings in the selective angiograms but were informed about the location of a prior intervention, such as PTCA or bypass surgery, including stenting or a bypass procedure. In each examination the reviewer was asked to evaluate between one and five coronary arteries or bypasses of interest. The number of vessels of interest depends on how many sites of interventions must be controlled.

Each target vessel, whether it was a native artery, a side branch or a bypass, was divided into three segments, including the distal parts. The procedure is not identical to the system of the American Heart Association (American Heart Association, 1975). For each segment the clinician was asked to provide a rating as follows: (*a*) no stenosis, (*b*) a hemodynamically non-significant stenosis with $< 70\%$ reduction in diameter, (*c*) a hemodynamically significant stenosis with $\geq 70\%$ reduction in diameter or (*d*) an occlusion. For the calculation of the sensitivity and the specificity, (*a*) and (*b*) were regarded as 'no stenosis' and (*c*) and (*d*) as 'stenosis'. Additionally, the reviewers used category (*e*) for segments that were well suited for evaluation (++), category (*f*) for segments that were of fair quality for evaluation (+) and category (*g*) for segments that were impossible to evaluate (−). Categorizations as (*e*), (*f*) and (*g*) were regarded as subjective, and the results were not suitable for quantitative analysis.

Another independent investigator analyzed the selective angiograms of 52 of these 60 patients in the same way. He followed protocols from the investigations and angiographic sequences. His interpretations were compared with the interpretations of the selective angiograms provided by various physicians located at the hospital where the procedure was performed.

In 354 segments of the target vessels, 34 stenoses were identified by both the independent investigator and the local angiographers, and 18 stenoses were identified by only one of the two. Nevertheless, the data of the local angiographers were used as the 'gold standard' against which the intravenous angiograms were evaluated.

3. Results

Since all patients had previously undergone a coronary angiogram, an allergic reaction to the contrast agent was not a problem; in a few cases medication was used to prevent such a reaction. There were no complications, major or minor, related to the procedure in any of the 379 patients, and hospitalization was never required.

Although images after injection into the superior vena cava have better quality than those after injection into the brachial vein, most injections were performed directly into an antecubital vein to diminish patient anxiety.

Coronary arteries down to 0.8 mm in diameter were imaged. Good image quality was shown for the RCA [certain diagnosis proximal of the crux cordis (bifurcation)], the LAD (certain diagnosis beyond the bifurcation of the left main) including the *D*1-branch, and all ACVBs and IMA-ACBs, as well as stents in the RCA, the LAD and bypasses. There was good visualization of the anastomoses (connection of the bypass to the native coronary artery) of RCA-ACVBs, LAD-ACVBs, *D*1-branch ACVBs and IMA-ACBs. Superposition problems may arise at anastomoses of ACVBs to the diagonal branch and *M*-branches of the Cfx. Because of superposition with the left atrium, left ventricle or aorta, the image quality of the ostium of the RCA and the Cfx were inadequate without image processing. The processing yielded good results for the ostium, for the center segment of the Cfx and often for *M*1. The visibility of the proximal segment of the Cfx was limited, as was the visibilty of the distal part of the Cfx in about 50% of the procedures in which the Cfx was a target vessel. There was inadequate image quality for the left main coronary artery owing to superposition with the aorta and suboptimal projection angles. However, the left main was not a target vessel in any of the subjects and it is expected that this problem can be overcome by different angulation. Examples of angiograms are presented in Figs. 3–6.

Data on all 225 examinations are presented. The results of the five independent reviewers for the sensitivity and specificity of 60 patients, including the 95% confidence intervals (CI), are presented in Table 1. The predictive values are given in Table 2. The values for all target vessels are combined.

The results (mean) for the sensitivity of the method for bypasses alone is higher than that for all target vessels: 68% *versus* 48%. However, the confidence intervals are huge if the sensitivity *etc.* are calculated for single arteries and bypasses. As an example, the data from one reviewer are provided in Table 3.

The large confidence intervals in Tables 1–3 show that only statistical approximations can be provided for the method. Two facts emerge:

(i) The reviewers had extensive prior experience in the interpretation of selective coronary angiograms, but no experience with the interpretation of intravenous angiograms. This fact may explain why the degree of the stenosis was often underestimated by the intravenous method. Most stenoses were identified by both methods, but often in intravenous angiograms the same stenosis was interpreted as $< 70\%$ and in selective angiograms as $\geq 70\%$, which resulted in a relatively low sensitivity.

(ii) The data from all reviewers have high negative predictive values, showing that the method gives very good results for the exclusion of stenoses. Because there were only 47 stenoses in 473 segments in this unselected sample of follow-up patients, these negative predictive values are important findings.

Table 1
Sensitivity and specificity for intravenous angiograms from different reviewers.

All numbers are pecentages. UE denotes unevaluable target vessels. 60 patients.

Reviewer	Sensitivity	CI	Specificity	CI	UE
1	58	43–68	98	97–99	6
2	79	66–88	93	91–94	3
3	30	19–40	99	97–99	7
4	26	13–36	99	98–100	13
5	44	26–60	97	95–98	12

Table 2
Positive and negative predictive values for intravenous angiograms from different reviewers.

All numbers are percentages. UE denotes unevaluable target vessels. 60 patients.

Reviewer	Positive predictive value	CI	Negative predictive value	CI	UE
1	75	56–88	96	95–97	6
2	54	46–61	97	96–99	3
3	83	52–97	94	93–94	7
4	70	37–92	94	93–95	13
5	53	31–72	96	94–97	12

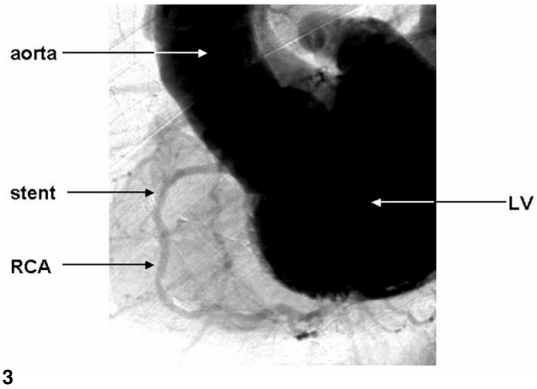

Figure 3
An intravenous angiogram of a 72-year-old male in the LAO 60° projection. Target: RCA with stent. Diagnosis: stent without pathological findings, in RCA vessel wall irregularities.

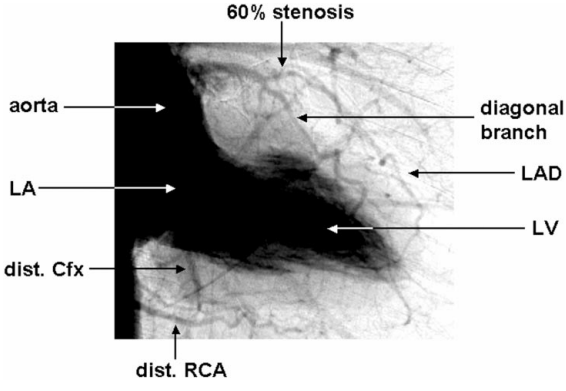

Figure 4
An intravenous angiogram of a 69-year-old female in the RAO 30° projection. Target: LAD. Diagnosis: 60% stenosis distal of *D*1, otherwise without pathological findings.

Table 3
Sensitivity and specificity from intravenous angiograms for all segments of the different target vessels including side branches.

UE denotes unevaluable target vessels. Reviewer 2. 60 patients.

Target	Sensitivity	CI	Specificity	CI	UE
LAD	15/16 (94%)	70–100%	112/125 (90%)	87–90%	2%
RCA	13/19 (68%)	47–85%	115/125 (92%)	89–94%	0%
Cfx	0/1 (0%)	0–87%	38/41 (93%)	92–95%	18%
Sum (native)	28/36 (78%)	63–89%	265/291 (91%)	89–92%	4%
Bypass	9/11 (82%)	52–97%	116/121 (96%)	93–97%	0%
Sum (total)	37/47 (79%)	66–88%	381/412 (93%)	91–94%	3%

The data for evaluability are given in Table 4. They show large discrepancies among the reviewers.

4. Discussion

In the past two decades efforts have been made to image coronary arteries non-invasively, with the intention of reducing the need for hospitalization, eliminating the hazards associated with intra-arterial manipulations, and reducing radiation exposure. Non-invasive or minimally invasive techniques must be safe, easy to perform, rapid, suitable for outpatient use and cost-effective. The image quality should be high. We believe that synchrotron-radiation angiography holds promise as such a method.

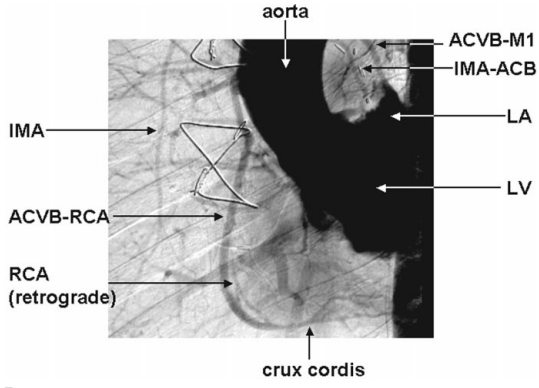

Figure 5
An intravenous angiogram of a 60-year-old male in the LAO 30° projection. Target: ACVB to RCA. Diagnosis: ACVB without pathological findings, RCA retrograde filled (about 3 cm) and distal of the anastomose patent.

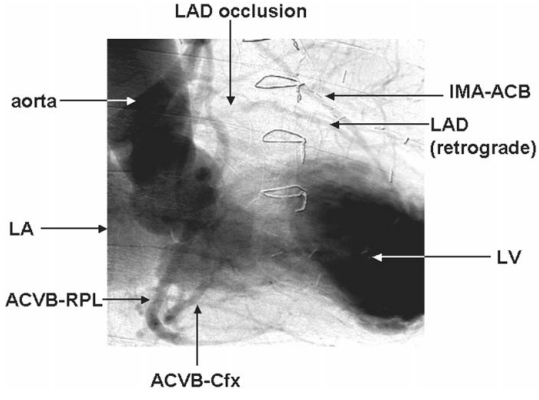

Figure 6
An intravenous angiogram of a 45-year-old male in the RAO 45° projection. Target: IMA-ACB to LAD. Diagnosis: IMA-ACB without pathological findings, LAD occlusion in the proximal part, retrograde filled and distal of the anastomose patent.

The results of the described study demonstrate the feasibility and safety of the method and its ability to provide useful information as to its diagnostic accuracy. In most instances, the method allows the evaluation of most segments of the coronary arteries and their side branches, as well as of bypasses and stents.

The quality of the images depends to a large extent on the projection angle. Most problems with unevaluable segments arise from superposition on the left ventricle, the aorta, pulmonary veins, edges of ribs or the spine. Other problems arise from a low signal-to-noise ratio in overweight patients or those with a low cardiac output, from imprecise measurement of the transit time, and from malpositioning. Optimal projections for good image quality can be found for the RCA, LAD and bypasses. Suitable projection angles have not as yet been found for the left main and part of the left circumflex. Sophisticated image-processing algorithms are now being studied for use on these vessel segments (Jung *et al.*, 1999).

While the superposition problem is a remaining challenge, intravenous coronary angiography has made critically important advances. The problem of the marked dilution of the contrast agent before it enters the arteries has been solved by the dichromographic subtraction method. Furthermore, problems arising from rapid cardiac motion have been overcome because the images, recorded with brief exposure times, are recorded simultaneously.

The images categorized as 'unevaluable' in Table 4 were analyzed for features that suggest improvements in the approach. Preliminary calculations suggest that the number of unevaluable segments can be reduced from 20% to about 5% if the improvements described below in this paragraph are performed. Furthermore, a considerable number of the (+) segments can be expected to become (++). Such modifications should also improve the predictive values, the sensitivity, and the specificity of the method. For example, the left main, the proximal part of the LAD and the Cfx should be imaged in diastole rather than in systole. In the present study the images were recorded in endsystole to avoid superposition of the left ventricle. However, cardiac motion is much slower in the diastolic phase, and this fact can be taken advantage of in the line-scan procedure. Flushing with saline solution should increase the concentration of the contrast material. Injection into the superior vena cava should be employed in obese patients with long transit times. Slight changes of the projection angle and the timing of the cardiac cycle between the single scans could help to overcome the problems from artefacts. Increasing the skin-entry dose to that of selective coronary angiography or increasing the amount of contrast agent would increase the signal-to-noise ratio in the images. In addition, several improvements in the image-processing algorithms are now planned. While these and other improvements are relatively easy to achieve, the precise determination of the transit time, which is very important for the method, remains a problem. Sudden changes of the transit time are not yet well understood.

The method must be compared with selective coronary angiography and with other competing methods, such as MRI, EBCT and MSCT.

As no complications have occurred during or following the investigations to date, and no hospitalization was necessary, the new method can be regarded as a purely ambulatory one with correspondingly low costs for each procedure. The acceptance by patients has been extremely high, because of the method's simplicity, the diminished radiation exposure and the reduced risk.

The intravenous injection does not distort the size of the coronary arteries, whereas the selective intra-arterial method subjects the vessels to sudden increases in pressure. In addition, calcification in the arterial wall, which can lead to false-positive interpretations with the conventional intra-arterial approach, presents no problem with the dichromographic method, which eliminates signals arising from calcium. This fact calls into question the use of the selective coronary angiographic approach as a reference standard. On the other hand, the arterially invasive approach has the advantage of allowing for a therapeutic intervention, such as angioplasty or stent placement, during the procedure.

Table 4
Evaluability ratings by different clinicians for various segments of vessels recorded by the intravenous method.

All numbers are percentages. (−) = unevaluable, (+) = fairly evaluable, (++) = good and certainly evaluable (60 patients).

Reviewer	(−)	(+)	(++)
1	18	30	52
2	11	45	44
3	8	18	74
4	31	44	25
5	31	40	29
Mean	20	35	45

The high negative predictive values are an important result of the study, because significant stenoses can be excluded with confidence. In the case of high-grade stenoses and complete occlusions, an additional selective coronary angiography is required. During that procedure a control of the determined degree of the stenosis and an eventual intervention is performed. The disadvantage of having only two views for an intravenous investigation could be overcome without an increase of the dose to the patient by using different projection angles for the single scans of one investigation run, if the change in angle is restricted to the range $\sim$5–10°. Intravenous and selective coronary angiography both have the limitation that they are contour methods, and information about the cross-sectional structure of the vessel wall, as provided by intravascular ultrasound, is not available.

In contrast to MRI, EBCT and MSCT, the evaluation of the peripheral parts of coronary arteries is not a problem for the synchrotron-radiation intravenous method, because the spatial resolution is higher by a factor of 3–4 and, therefore, the accuracy for diagnosis is superior to that of the other techniques. In the present study there was no relevant difference for the sensitivity, specificity and predictive values if the distal parts of the coronary arteries were included or not.

Arrhythmia and respiratory motion do not lead to blurring in the images, which does occur in the competing methods, and cardiac motion has much less of an effect, because the line-to-line interval in the images is only 0.8 ms. Therefore, a far higher degree of patient cooperation is required for the competing methods.

Because metal does not result in image dropouts, such as occur in MRI, the intravenous method is suitable for diagnostic evaluation in the presence of stents and bypasses, particularly in IMA-ACBs. Calcification is no problem for the present method, in contrast to EBCT, MSCT and to a lesser extent MRI, in which calcification leads to local signal deletion and, therefore, is a frequent reason for false-negative and false-positive results. In addition, signals from adjacent tissue, such as myocardium or fat, which influence MRI interpretation, are eliminated by the subtraction algorithms. MRI, of course, does not expose the patient to ionizing radiation, and MRI provides information not only about morphology but also about myocardial perfusion, viability and cardiac function.

Myocardial perfusion can readily be calculated with the synchrotron-radiation intravenous method from single scans that have a

relative temporal interval of about 2 s. New software is under development for this purpose (Dix *et al.*, 2003).

The sensitivity, specificity and predictive values for the detection of complete occlusions and high-grade stenoses in the presented study are comparable with the results of studies for MRI (Duerinckx & Umann, 1994; Woodard *et al.*, 1998; Huber *et al.*, 1999; Stuber *et al.*, 1999; Lethimonnier *et al.*, 1999), EBCT (Achenbach *et al.*, 1997, 1998; Raggi *et al.*, 2000) and MSCT (Cline *et al.*, 2000; Achenbach *et al.*, 2000; Nieman *et al.*, 2001), especially if the portion of non-evaluable vessels is taken into account. It must be stressed that in our study all parts of the native coronary arteries, side branches and bypasses are included, whereas the other studies include only proximal and middle segments of the main coronary arteries. Furthermore, the goals of the studies are different. In our case, the application is for follow-up rather than for primary diagnosis. All studies, irrespective of which of the four methods are applied, are hampered by very large confidence intervals and, therefore, provide trends rather than exact values. For exact values, some thousands of patients must be investigated. In addition, using selective coronary angiography as a 'gold standard' is problematic, as already discussed.

In the present study the patients were not required to undergo the intravenous and the selective investigation within a specific time interval, as would be preferred for optimal evaluation. Of the 230 patients, 91 declined to give consent for a selective arteriographic procedure on the basis of the information that the intravenous study showed no significant stenoses. Only 60 of the 230 patients had the two investigations within eight weeks. These images were used for the evaluation process, despite the relatively long interval between the two studies.

Overall the studies show that none of the four methods will replace selective coronary angiography, but they could be used for several applications with low risk and with benefits to some patients. One obvious application for the new intravenous method is the assessment of stents. After the improvements mentioned above have been implemented, and with carefully selected projection angles for the stents of interest, there appears to be high diagnostic value of the method in this setting. Another attractive application could be the early and late post-operative evaluation of the effects of bypass surgery.

It is important that, in the future, clinicians have detailed training in image evaluation by the intravenous method, prior to their use of it as a diagnostic method.

A new gadolinium-containing contrast agent with a higher concentration (157 mg ml^{-1} of gadolinium) is now available. After adjustments to the monochromator and the detector, high-dose gadolinium might prove to be a valuable alternative contrast agent. The *K*-edge of gadolinium is at 50.2 keV; the absorption length in soft tissues of such monochromatic X-rays would increase from 2.1 cm to 3.1 cm. Whether its use would result in a better image quality at the same or lower radiation dose needs to be established by phantom and animal studies (Fiedler *et al.*, 2000; Lohmann, Dix *et al.*, 2003).

Currently, no commercially available system is suitable for intravenous iodine-dichromographic coronary angiography. Approaches based on channeling radiation or on lasers have not succeeded in reaching the intensity of monochromatic X-ray radiation required (Genz *et al.*, 1990; Reich *et al.*, 2000).

A feasibility study of a small storage ring as a compact source was prepared at DESY (Brinker *et al.*, 2000). The proposed ring achieves a sufficient intensity at 33 keV, and this study could serve as the basis for an industrial plan that should allow a reduction in the initial costs. A cost-benefit analysis must be performed in the near future. For these calculations several other medical applications of synchrotron radiation that are under development (Arfelli, 2000) should be taken into consideration. The source could be installed in a large medical center.

A rough estimation showed that the costs per investigation could be lower than those for selective coronary angiography, provided that sufficient patient examinations are undertaken.

Assuming that a stent is implanted in 57% of coronary interventions (Mannebach *et al.*, 2000), and that in 30% of these there is a need for follow-up assessment of the status of the stent's function, we would conclude that there are 96000 patients per year in Germany who would be potential candidates for study in such a center. Therefore, a substantial number of invasive coronary angiographic studies that have negative results could be replaced by minimally invasive outpatient examinations.

APPENDIX *A*

ACVB (aorto coronar vein bypass): A bypass between the aorta and the native coronary artery, made from a vein.

Anastomose: The site where the bypass is connected to the native coronary artery.

Angiography: A method for the visualization of vessels in the body with the help of an introduced X-ray-absorbing contrast agent and an X-ray unit.

Angioplasty: See PTCA.

Antecubital vein: A vein in front of the elbow.

Anti-anginal and low-dose aspirin medication: Medication against chest pain, *e.g.* aspirin (acetylic salicylicacid), a blood platelet aggregation inhibitor.

Aorta: The central body artery, which is next to the left ventricle of the heart. The coronary arteries escape from the aorta.

Atrium: A heart chamber (left and right) in front of the main chamber.

Bodymass index: The weight of a person divided by the square of the height (units of kg m^{-2}). A normal bodymass index falls in the range 20–25 kg m^{-2}.

Bolus: The volume of a fluid in a vessel of short length after fast injection of this fluid (about 2 s in the described method).

Brachial vein: A vein in the arm.

Bypass graft: See ACVB and IMA-ACB.

CC projection (craniocaudal or caudiocranal projection): A projection at a certain angle relative to the horizontal axis of the patient.

Cfx (circumflex coronary artery): One of the three main coronary arteries.

Contrast agent: An X-ray-absorbing dye that is injected into the vessels of interest. The described method used an iodine-containing contrast agent.

Coronary arteries: Arteries that supply the heart with blood.

Crux cordis: Bifurcation of the RCA.

Diastolic phase: The phase in which the heart chamber is filled and at rest.

Distal part: The end part of a vessel.

*D*1-branch: The first of the diagonal branches, *i.e.* side branches of the LAD.

EBCT (electron beam computed tomography): An ultrafast CT method in which the detector and source are not moved but an electron beam sweeps over a cathode of 180°.

ECG trigger: A trigger from the electrocardiogram, which allows a measurement in a fixed heart phase.

Ejection fraction: The blood volume ejected from the left ventricle during one heart cycle compared with the ventricle volume (units %).

Flush: An additional injection of a saline solution immediately after the injection of the contrast agent.

French (F): Length scale; 1 F = 0.33 mm.

IMA-ACB (aorto coronar bypass with the internal mammary artery): An artery that is behind the breastbone is connected as a bypass to the coronary artery.

Indocyanine green: A green organic fluid that can be identified by a densitometer.

Intravenous coronary angiography: Coronary angiography in which the contrast agent is injected into a vein. Also named non-invasive or minimally invasive coronary angiography.

Introducer sheath: A plastic cannula that is put into a vessel and allows the injection of a contrast agent or the introduction of a catheter.

Invasive coronary angiography: Coronary angiography in which the contrast agent is injected into an artery. Also named selective coronary angiography.

LAD (left anterior descending coronary artery): One of the three main coronary arteries.

LAO (left anterior oblique) projection: A projection under a certain angle relative to the vertical axis of the patient.

Left main: Part of the left coronary artery next to the aorta. The left main splits up into the LAD and the Cfx.

Minimally invasive technique: See Intravenous coronary angiography.

MRI (magnetic resonance imaging): A slice technique that allows the presentation of images of volumes without the use of X-rays but with high magnetic fields.

MSCT (multislice beam computed tomograph): A fast CT method where four or more slices of a volume are imaged in parallel with the spiral-CT technique.

*M*1-branch: The first of the marginal branches, *i.e.* side branches of the Cfx.

Negative predictive value: The conditioned probability that a disease does not exist if a certain test parameter is negative.

Non-invasive technique: See Intravenous coronary angiography.

Ostium: The entrance into a coronary artery that is directly at the aorta.

Perfusion: A measure of the blood supply of the heart muscle.

Peripheral intravenous injection: An injection into a vein of the arms or legs.

Positive predictive value: The conditioned probability that a disease exists if a certain test parameter is positive.

Protocol: A given procedure for the investigation of the patient.

PTCA (percutane transluminal coronary angioplasty): A technique to widen a narrowed vessel with the help of a balloon.

RAO (right anterior oblique) projection: A projection at a certain angle relative to the vertical axis of the patient.

RCA (right coronary artery): One of the three main coronary arteries.

Rotational atherectomy: The debulking of narrowings in a coronary artery with a high-speed rotating catheter.

RPL-branch: The distal branch of the right coronary artery.

R-wave: A spike-like wave in the curve of the ECG, which is optimal for a trigger.

Scaphoid fossa: The upper part of the external ear.

Selective coronary angiography: See Invasive coronary angiograph.

Sensitivity: The conditioned probability that for a patient with a disease a certain test parameter is positive.

Single-vessel disease: Disease in one of the three coronary arteries.

Specificity: The conditioned probability that for a patient without a disease a certain test parameter is negative.

Stenosis: A site in an artery where it is narrowed.

Stent: A tube of mashed metal that is put into an artery after PTCA in order to keep the artery wide.

Superior vena cava: The central vein that is next to the right atrium.

Systolic phase: The phase when the heart chamber is compressed and emptying.

Transit time: The time between the injection of the contrast agent and its arrival in the coronary arteries.

Unstable angina pectoris: Heart pain of new onset or increasing intensity and duration.

Ventricle: The main heart chamber (left and right).

Over the years 14 physicians from the University Hospital Hamburg-Eppendorf (UKE) and the Heart Center Bevensen, as well as 35 physicists, computer scientists and engineers from HASYLAB at DESY, the Physics Department of the University of Siegen (UniSI), and the Physics Department of the University of Hamburg (UniHH), were involved in the project, including H. J. Besch (UniSI), W. Bleifeld (UKE; deceased), O. Dünger (HASYLAB), K. Engelke (UniHH), C.-C. Glüer (UniHH), W. Graeff (HASYLAB), U. Großmann (UniSI), G. Heintze (HASYLAB), J. Heuer (HASYLAB), K. H. Höhne (UKE), C. P. Höppner (UniHH), H. Hultschig (HASYLAB), S. Iksal (UniSI), G. Illing (HASYLAB), H. Jabs (UniHH), D. Jowanowich (UniSI), M. Jung (HASYLAB), B. Kaempf (UniHH), J. Knabe (HASYLAB), H. Krieger (UniSI), R. Langer (UniSI), I. Makin (Fachhochschule Hamburg-Bergedorf), T. Meinertz (UKE), R. H. Menk (HASYLAB/UniSI), M. Mishima (UKE), T. Möchel (UniHH), W. Neef (UniSI), R. Reumann (HASYLAB), C. Rust (UKE), H. W. Schenk (UniSI), L. Schildwächter (HASYLAB), L. Schlüter (UKE), S. Schröder (UKE), G. Seiffert (UKE), P. Steiner (UKE), K.-H. Stellmaschek (HASYLAB), U. Tafelmeier (HASYLAB/UniSI), M. Wagener (UniSI), A. H. Walenta (UniSI), T. Wroblewski (HASYLAB) and H. C. Xu (UniSI). Their contributions to the method and to the system are gratefully acknowledged. We are grateful to Tilman Jaup MD (Bad Bevensen), Hansjörg Just MD (Freiburg), Thomas Meinertz MD (Hamburg), Klaus von Olshausen MD (Hamburg) and Wilhelm Rutishauser MD (Geneve) for the image evaluation. We thank Miss Gabriele Frost and Miss Nicole Seidler for technical assistance during the patient investigations. Edward Rubenstein MD (Stanford University) reviewed the manuscript and we thank him for his suggestions. The work was supported in part by Werner-Otto-Stiftung, Hamburg, Siemens AG, Medizinische Technik, Region Nord and the Bundesministerium für Bildung, Forschung und Technologie under contract No. 05330-GKA 9.

References

Achenbach, S., Moshage, W. & Bachmann, K. (1997). *Circulation*, **96**, 2785–2788.

Achenbach, S., Moshage, W., Ropers, D., Nossen, J. & Daniel, W. G. (1998). *N. Engl. J. Med.* **339**, 1964–1971.

Achenbach, S., Ulzheimer, S., Baum, U., Kachalreiss, M., Ropers, D., Giesler, T., Bautz, W., Daniel, W. G., Kalender, W. A. & Moshage, W. (2000). *Circulation*, **102**, 2823–2828.

American Heart Association (1975). *Circulation*, **51**, Suppl. 5–40.

Arfelli, F. (2000). *Nucl. Instrum. Methods Phys. Res. A*, **454**, 11–25.

Brinker, F., Febel, A., Hemmie, G., Liu, N., Nesemann, H., Schmitz, M., Tesch, K. & Wipf, S. (2000). Internal Report DESY M00-01. DESY, Hamburg, Germany.
Cline, H., Coulam, C., Yavuz, M., Rubin, G. D., Edic, P., Pan, T., Shen, Y., Avila, L., Turek, M., Iatrou, M., Luree, A., Ishaque, N. & Senzig, R. (2000). *Circulation*, **102**, 1589–1590.
Dill, T., Dix, W.-R., Hamm, C. W., Jung, M., Kupper, W., Lohmann, M., Reime, B. & Ventura, R. (1998). *Eur. J. Phys.* **19**, 499–511.
Dill, T., Job, H., Dix, W.-R., Ventura, R., Kupper, W., Hamm, C. W. & Meinertz, T. (2000). *Z. Kardiol.* **89**, Suppl. 1, I27–I33.
Dix, W.-R. (1995). *Prog. Biophys. Mol. Biol.* **63**, 159–191.
Dix, W.-R., Kupper, W., Lohmann, M., Reime, B. & Rubenstein, E. (2003). In preparation.
Duerinckx, A. J. & Umann, M. K. (1994). *Radiology*, **193**, 731–738.
Elleaume, H., Fiedler, S., Esteve, F., Bertrand, B., Charvet, A. M., Berkvens, P., Berruyer, G., Brochard, T., Le Duc, G., Nemoz, C., Renier, M., Suortti, P., Thomlinson, W. & Le Bas, J. F. (2000). *Phys. Med. Biol.* **45**, L39–L43.
Fiedler, S., Elleaume, H., Le Duc, G., Nemoz, C., Brochard, T., Renier, M., Bertrand, B., Esteve, F., Le Bas, J.-F., Suortti, P. & Thomlinson, W. (2000). *Proc. SPIE*, **1991**, 96–103.
Genz, H., Gräf, H.-D., Hoffmann, P., Lotz, W., Nething, U., Richter, A., Kohl, H., Weickenmeier, A., Knüpfer, W. & Sellschop, J. P. F. (1990). *Appl. Phys. Lett.* **57**, 2956–2958.
Huber, H., Nikolaou, K., Gonschior, P., Knez, A., Stehling, M. & Reiser. M. (1999). *Am. J. Roentgenol.* **173**, 95–101.
ICRP (1990). *Recommendations of the International Commission on Radiological Protection*, ICRP Publication 60, *Annals of the ICRP*. Oxford: Pergamon Press.
Illing, G., Heuer, J., Reime, B., Lohmann, M., Menk, R. H., Schildwächter, L., Dix, W.-R. & Graeff, W. (1995). *Rev. Sci. Instrum.* **66**, 1379–1381.
Jacobson, B. (1953). *Acta Radiol.* **39**, 437–452.
Jung, M., Dill, T., Dix, W.-R., Hamm, C. W., Kupper, W., Lohmann, M., Reime, B. & Ventura R. (1999). *IEEE Comput. Cardiol.* **26**, 359–362.
Lethimonnier, F., Furber, A., Morel, O., Geslin, G. D., L'Hoste, P., Caron-Poitreau, C. & Le Jeune, J. J. (1999). *Magn. Reson. Imaging*, **17**, 1111–1120.
Lohmann, M., Besch, H. J., Dix, W.-R., Dünger, O., Jung, M., Menk, R. H., Reime, B. & Schildwächter, L. (1998). *Nucl. Instrum. Methods Phys. Res. A*, **419**, 276–283.
Lohmann, M., Besch, H. J., Dix, W.-R., Metge, J. & Reime, B. (2003). *Nucl. Instrum. Methods Phys. Res.* In the press.
Lohmann, M., Dix, W.-R., Graeff, W. & Reime, B. (2003). In preparation.
Mannebach, H., Hamm, Ch. & Horstkotte, D. (2000). *Z. Kardiol.* **89**, 976–984.
Nieman, K., Oudkerk, M., Rensing, B. J., von Ooijen, P., Munne, A., van Geuns, R.-J. & de Feyter, P. J. (2001). *Lancet*, **357**, 599–603.
Ohtsuka, S., Sugishita, Y., Takeda, T., Itai, Y., Tada, J., Hyodo, K. & Ando, M. (1999). *Br. J. Radiol.* **72**, 24–28.
Raggi, P., Callister, T. Q., Cooil, B., He, Z.-X., Lippolis, N. J., Russo, D. J., Zelinger, A. & Mahmarian, J. J. (2000). *Circulation*, **101**, 850–855.
Reich, C., Gibbon, P., Uschmann, I. & Förster, E. (2000). *Phys. Rev. Lett.* **84**, 4846–4849.
Rubenstein, E., Hofstadter, R., Zeman, H. D., Thompson, A. D., Otis, J. N., Brown, G. S., Giacomini, J. C., Gordon, H. J., Kernoff, R. S., Harrison, D. C. & Thomlinson W. (1986). *Proc. Natl Acad. Sci. USA*, **83**, 9724–9728.
Shanghai National Synchrotron Radiation Center (1999). SSRF Beamline Conceptual Design Report. Shanghai National Synchrotron Radiation Center, Shanghai, People's Republic of China.
Stuber, M., Botnar, R. M., Danias, P. G., Sodickson, D. K., Cauteren, M. V., Kissinger, K. V. & Manning, W. J. (1999). *J. Am. Collect. Cardiol.* **34**, 524–531.
Woodard, P. K., Li, D., Haacke, E. M., Dhawale, P. J., Kaushikkar, S., Barzilai, B., Braverman, A. C., Ludbrook, P. A., Weiss, A. N., Brown, J. J., Mirowitz, S. A., Pilgram, T. K. & Gutierrez, F. R. (1998). *Am. J. Roentgenol.* **170**, 883–888.
Zeman, H. D. (1991). *Handbook on Synchrotron Radiation*, Vol. 4, edited by S. Ebashi, M. Koch & E. Rubenstein, pp. 697–718. New York: North-Holland/Elsevier.

Received 5 July 2002 • Accepted 22 January 2003